The iron regulatory proteins are defective in repressing translation via exogenous 50 iron responsive elements despite their relative abundance in leukemic cellular models

Emmanuel Pourcelot, Marine Lénon, Peggy Charbonnier, Fiona Louis, Pascal Mossuz, Jean-Marc Moulis

The iron regulatory proteins are defective in repressing translation via exogenous 50 iron responsive elements despite their relative abundance in leukemic cellular models

Emmanuel Pourcelot,[abc] Marine Lénon,[a] Peggy Charbonnier,[d] Fiona Louis,[d] Pascal Mossuz[bc] and Jean-Marc Moulis[ad]

In animal cells the specific translational control of proteins contributing to iron homeostasis is mediated by the interaction between the Iron Regulatory Proteins (IRP1 and IRP2) and the Iron Responsive Elements (IRE) located in the untranslated regions (UTR) of regulated messengers, such as those encoding ferritin or the transferrin receptor. The absolute concentrations of the components of this regulatory system in hematopoietic cells and the ability of the endogenous IRP to regulate exogenous IRE have been measured. The IRP concentration is in the low μM (10^{-6} M) range, whereas the most abundant IRE-containing messenger RNA (mRNA), *i.e.* those of the ferritin subunits, do not exceed 100 nM (10^{-7} M). Most other IRP mRNA targets are around or below 1 nM. The distribution of the mRNA belonging to the cellular iron network is similar in human leukemic cell lines and in normal cord blood progenitors, with differences among the cellular models only associated with their different propensities to synthesize hemoglobin. Thus, the IRP regulator is in large excess over its presently identified regulated mRNA targets. Yet, despite this excess, endogenous IRP poorly represses translation of transfected luciferase cDNA engineered with a series of IRE sequences in the 5′ UTR. The cellular concentrations of the central hubs of the mammalian translational iron network will have to be included in the description of the proliferative phenotype of leukemic cells and in assessing any therapeutic action targeting iron provision.

Introduction

The translation of messenger ribonucleic acids (mRNA) can be regulated by many mechanisms that have been separated between global control, whereby the translation rate of the transcriptome as a whole is modulated *via* the translational machinery, and specific control in which features of a given subset of mRNA (*cis*-elements) is targeted by *trans*-regulatory molecules.[1] Among the latter, messenger ribonucleoproteins and micro-RNA (miRNA) provide means to finely tune translation of targeted mRNA, and their involvement in a large number of cancers emphasizes their importance in the maintenance of cellular balance between proliferation and differentiation.

One of the most representative and better known examples of specific translational control is afforded by the Iron Regulatory Proteins (IRP1 and IRP2) interacting with stem-loop structures in

[a] *Univ. Grenoble Alpes, Inserm U1055, Laboratory of Fundamental and Applied Bioenergetics (LBFA) and SFR BEeSy, 38000 Grenoble, France*
[b] *CHU Grenoble, Laboratoire d' Hématologie, Institut de Biologie et Pathologie, Grenoble, France*
[c] *Univ. Grenoble Alpes, TIMC – Imag CNRS 5525, Grenoble, France*
[d] *Commissariat à l'Energie Atomique et aux Energies Alternatives – Biosciences & Biotechnology Institute of Grenoble (BIG), France.*
E-mail: jean-marc.moulis@cea.fr

the UTR (untranslated regions) of some messengers in animals.[2] These *cis*-elements are called Iron Responsive Elements (IRE).† The regulated mRNA encode proteins directly involved in iron handling at the cellular level, such as transferrin receptor 1 or ferritin. Other targets of IRP are more remotely associated with iron, as they participate in progress of the cell cycle or adjustment to variations of available oxygen.[3] Over the last three decades a lot of qualitative information has been gathered on this system, at all relevant levels of analysis, from molecules[4] to model animals[5] and human pathologies.[6] These data turned the IRP/IRE system into an archetype of translational control by protein–mRNA interaction.[7] However, the quantitative importance of the IRP/IRE system is rarely evaluated in a given biological context, despite the phenotypical changes observed upon its dysfunction.[3,5]

Improved understanding of the role of iron homeostasis in normal and pathological hematopoiesis is required since normal erythropoiesis has been known for a long time to rely on efficient iron provision, but more recent data have suggested that abundant iron may contribute to the leukemic process, *e.g.* ref. 8. Indeed, iron chelation therapy, together with vitamin D administration, has been shown to contribute to improvement of particular leukemic patients with increased survival and improved cellular differentiation.[9] Thus iron homeostasis in normal and pathological hematopoiesis represents a prospective therapeutic target, and a robust and quantitative description of iron homeostasis in different conditions is required to reach this target.[10] Toward this aim, the cellular concentrations of most of the proteins building the IRP network and the ability of the endogenous IRP to regulate exogenous IRE have been measured here in hematopoietic progenitors and some of their cellular models.

Experimental

Reagents

All reagents were obtained from Sigma-Aldrich unless stated otherwise. Recombinant human IRP 1 and 2 were obtained and assayed as previously detailed.[11–13]

Cell lines and treatments

The cell lines used in the present study originated from the ATCC biological resource. The human myeloid leukemia KG1 (derived from a patient with erythroleukemia that evolved into acute myelogenous leukemia) and K562 (from a patient diagnosed with chronic myelogenous leukemia) cells were grown in RPMI-1640 medium, supplemented with 10% fetal bovine serum (BioWest, origin: South America, lot containing 1.7 mg of iron per l), 2 mM L-glutamine, 100 U of penicillin per ml and 0.1 mg streptomycin per ml at 37 °C with 5% CO_2. Viable cells were determined by Trypan blue staining and quantified with a Luna™ counter (Logos). Cells were starved for iron as previously detailed.[13] The chelating agent desferrioxamine (DFO) was added for 24 hours at 200 μM. Treatments with 1 μM cytosine arabinoside (cytarabine) that blocks mitosis by interacting with DNA and 200 μM hydroxyurea that inhibits ribonucleotide reductase were similarly carried out. Growth arrest was measured by cell cycle analysis with propidium iodide DNA labeling as reported previously,[13] on a LSR Fortessa™ cell analyzer (Becton Dickinson).

Hematopoietic progenitors

Hematopoietic progenitors were separated from cord blood using the CD34 surface marker. They were isolated from cord blood units by Ficoll-Hypaque density gradient centrifugation and $CD34^+$ progenitors were separated by immune-magnetic cell sorting (Miltenyi Biotec). Cord blood procedures were approved by the French Blood Service's Institutional Review Board, and informed consent for therapeutic and research use was obtained from the parents.

IRP activity measurement

IRP RNA-binding activities were measured by RNA Electrophoretic Mobility Shift Assays (REMSA) with 3 μg of total protein extracts. The minimal sequence of human ferritin H-chain IRE was biotin-labeled with biotinylated cytidine (bis)phosphate using T4 RNA ligase (Thermo Scientific). The IRE–IRP reaction was carried out as previously described[11,12] and the complexes were separated on non-denaturing 4% PAGE in 0.5× TBE, transferred onto hybond N^+ membrane (GE Healthcare Life Sciences), and the biotinylated bands were detected after interaction with the streptavidin–horseradish peroxidase conjugate by the chemiluminescent luminol product. To unveil all IRP1 activity (conversion of the aconitase form to the IRP binding one), 2% β-mercaptoethanol (2ME) was added to the reaction. Quantification of the signals was done with the Image J software (v1.47, Wayne Rasband, Research Services Branch, National Institute of Mental Health, Bethesda, Maryland, USA).

Western blotting

Ten to forty μg of total proteins were resolved by sodium dodecyl sulfate–polyacrylamide gel electrophoresis on 8% gels, and proteins were transferred to polyvinylidene difluoride membranes. The blots were saturated with 5% non-fat milk in phosphate buffered saline (PBS)-Tween 0.2% and probed overnight at 4 °C with antibodies (all produced in rabbit). Primary antibodies were raised against human IRP1[14] (dilution 1 : 500) and actin (1 : 250, Sigma Aldrich). IRP2 antibodies were from Everest Biotech (EB09488), Alpha Diagnostic (IRP21-A), Santa Cruz Biotechnology, Inc. (sc-33680), or home-made ones from the purified IRP2 specific domain:[12] the latter were validated in other cell systems.[15] Following three washes with PBS-Tween 0.2%, the blots were incubated with peroxidase-coupled goat anti-rabbit IgG (Bethyl) at a dilution of 1 : 5000 for 1 h at room temperature, followed by detection with the Pierce ECL western blotting substrate (Thermo Scientific). Recombinant human IRP1[11] was used for quantification in total protein extracts. Quantification of the signals was done as for REMSA results (see above).

† The plural is not indicated by 's' added to abbreviations throughout.

Measurements of mRNA concentrations

The experiments were designed and are reported below in agreement with the Minimum Information for Publication of Quantitative Real-Time PCR Experiments.[16] Total RNA was purified from cell lines using the NucleoSpin RNA II kit (Macherey-Nagel). In the case of $CD34^+$ progenitors, RNA was purified using the High Pure RNA isolation kit (Roche) and complementary DNA (cDNA) was synthesized using the Ovation PicoSL WTA System V2, powered by Ribo-SPIA technology (NuGEN). Complementary DNA from RNA purified from cell lines was synthesized using 1 μg of RNA with 200 units of modified Moloney Murine Leukemia virus reverse transcriptase (M-MuLV RT, Euromedex) and 0.5 μg of oligo$(dT)_{12\text{-}18}$ primer (Invitrogen) in 20 μl of 50 mM Tris–HCl pH 8.3, 50 mM KCl, 4 mM $MgCl_2$, 10 mM DTT, 1 mM dNTP, and 20 units of ribonuclease inhibitor. The obtained cDNA were diluted and the genes of interest were amplified by real time qPCR (C1000 Thermal Cycler CFX96, BioRad or Stratagene Mx3005 RT PCR System), using 2.5 μl of the diluted cDNA template, 0.2 μM of validated primers on each instrument (Table 1) and the HOT Pol EvaGreen qPCR Mix Plus (Euromedex) in 10 μl reaction volumes. Amplification was carried out for 15 min at 95 °C to activate the polymerase, followed by 40 cycles at 95 °C for 15 s, 60 °C for 20 s, and 72 °C for 20 s. Dissociation curves of the amplicons were recorded by heating between 55 and 95 °C.

The amounts of studied mRNA were referred to the gene of hypoxanthine guanine phosphoribosyl transferase (hPRT). The invariability of this gene was checked by running initial experiments with two other reference genes, the ribosomal protein lateral stalk subunit P0 (RPLP0) and glyceraldehyde-3-phosphate dehydrogenase (GAPDH).

Absolute quantification of mRNA

Absolute concentrations of transcripts were determined by spiking the samples at two key steps of RNA manipulation with non-mammalian mRNA of known concentrations. The latter were the mRNA of β-galactosidase (β-Gal, 3420 nt) and that of firefly luciferase (F-*luc*, 1929 nt) from available constructions (TriLink BioTechnologies, Inc, San Diego, CA, USA). First, one of these non-mammalian mRNA was added to the cell lysate just before RNA purification to later estimate the yield of this purification step. Then, a known amount (10 pg) of the second non-mammalian mRNA was added to the RT reaction to quantitatively refer the qPCR results to the absolute mRNA amounts of the transcripts of interest in the RT reaction. A calibration curve was determined for each of the β-Gal and F-*luc* mRNA by varying the amount added at these two steps. With this protocol, calibrating and unknown transcripts are processed in the same way from RNA purification downward. In separate qPCR experiments, it was checked that the C_q of the reference mRNA (hPRT, RPLP0, GAPDH) always fell within 1 unit between different PCR plates using the same cDNA matrix. In all selected experiments, this criterion was applied together with the absence of any amplified product in 40 cycles by

Table 1 Oligonucleotides used to amplify the cDNA of targeted genes

Gene	Symbol	Primer sequences forward/reverse	Amplicon size (bp)	PCR efficiency (%)	OIE[a]
Ferritin heavy chain	FTH1	CGAGGTGGCCGAATCTTCC GTTTGTGCAGTTCCAGTAGTGA	133	99.2	y
Ferritin light polypeptide	FTL	CAGCCTGGTCAATTTGTACCT CCAGTTCGCGGAAGAAGTG	113	101.1	n
Ferroportin	SLC40A1	CACAATACGAAGGATTGACCAGT ATCCCGAAATAAAGCCACAGC	107	93.5	y
5′-Amino levulinate synthase	ALAS2	CTACCCAAGGACCAAACTGTTC GACCAGGGAGCTAGGCAGAT	202	100.8	y
Aconitase 2 (mitochondrial)	ACO2	CCACTGTGACCATCTGATTGAA CACGCCATATTTGGCACCTG	117	81.7	y
Transferrin receptor	TFRC	ACCATTGTCATATACCCGGTTCA GGCCTTTGTGTTATTGTCAGCAT	115	96.5	n
Iron regulatory protein 1	ACO1	GATATGGGCGCTTACCATTTTCG GGCACACCCGTAAAGTCCTG	184	100.5	y
Iron regulatory protein 2	IREB2	CAATCCATCTGTCATGCTTGC GGTAATACTCCACTTGAACTGAGG	144	113.1	y
Heme oxygenase 1	HMOX1	CAGTGCCACCAAGTTCAAGC GTTGAGCAGGAACGCAGTCTT	122	92.5	n
Heme oxygenase 2	HMOX2	GGAGCGCAACAAGGACCAT TCCTCCCAGTTTTCACCAAAGA	114	100.5	y
Hemoglobin subunit alpha	HBA1	CTCTTCTGGTCCCCACAGACT GGCCTTGACGTTGGTCTTG	76	97.1	n
Hemoglobin subunit beta	HBB	CTCATGGCAAGAAAGTGCTCG AATTCTTTGCCAAAGTGATGGG	180	99.2	y
Hemoglobin subunit gamma	HBG	GGTGCAGGCTTCCTGGCAGA GCTCTGAATCATGGGCAGTGAGC	185	99.9	y
Beta galactosidase	BGAL	ACTATCCCGACCGCCTTA TAGCGGCTGATGTTGAACTG	172	98.9	n/a
Firefly luciferase	F-luc	ATGAACGTGAATTGCTCAACAG TAAAACCGGGAGGTAGATGAGA	201	101.5	n/a

[a] OIE: overlap intron-exon junction yes/no. n/a: not applicable.

omitting the RT enzyme. Other relevant information is provided in Table 1.

The concentrations of the transcripts in the samples were thus calculated with reference to the added mRNA of β-Gal or of F-*luc*. The ΔC_q method gave the relative amounts present in the qPCR reaction. These values were converted, by considering matrix dilution, to those present in the RT product using the mRNA quantity (say F-*luc*) added to the RT reaction. The amounts of mRNA of interest in the sample were then calculated based on the yield of the preparation as afforded by the second calibrating mRNA (say β-Gal), and referred to the known quantity of cells used in the experiment. The average volume of the cell types studied herein were estimated at 2.5 and 0.8 pL for K562 and KG1 cells, respectively,[13] which enables conversion of the values into the reported cellular concentrations. Of note, the results obtained by this double spiking procedure are in agreement with those generated by other methods.[17–20]

Cloning of regulatory IRE in pGL3-control

The IRE-bearing fragments listed in Table 2 were cloned in the pGL3-control plasmid (Promega) cleaved with *Hind*III and dephosphorylated with calf intestine alkaline phosphatase (MBI Fermentas) according to the manufacturer instructions. The restriction site lies on the 3′ side of the SV40 promoter and on the 5′ one of the *luc* coding sequence in this plasmid. The two oligonucleotides bearing the complementary IRE sequences of each studied mRNA were chemically synthesized (Eurofins MWG, Operon), and 2 nmol of each strand were phosphorylated with 20 u of T4 polynucleotide kinase (Euromedex, Souffelweyersheim, France) with 100 μM of ATP in 20 μl of reaction volume.

The phosphorylated duplex was inserted into the cleaved and dephosphorylated plasmid by ligation with T4 DNA ligase (MBI Fermentas) in a 1 : 5 plasmid : insert molecular ratio. Competent *E. coli* DH5α cells (Invitrogen) were then transformed by 50 fmol of the ligated plasmid, spread on Luria broth plates containing 75 μg ml^{-1} of ampicillin, and grown overnight at 37 °C.

To identify the plasmid constructions, colonies were picked and grown in Terrific Broth liquid medium (Gibco) with 100 μg ml^{-1} ampicillin. Plasmid DNA was purified (Plasmix kit, Talent Srl, Trieste, Italy), selected by restriction analysis for the presence of the insert, and eventually identified by sequencing. Plasmids with the IRE sequence in the correct orientation (IRE 5′ → 3′: plasmid IRE(+)) or its reverse complement (IRE 3′ → 5′ = ∼IRE: plasmid IRE(−)) were kept for further analysis.

Cell transfection and *in cellulo* measurement of IRE-regulated IRP activity

KG1 and K562 cells were transfected with the IRE(+) or IRE(−)-plasmid encoding firefly *luc* under the dependence of the inserted sequence, and a control of transfection (pGL4.75, Promega) at the 7 : 1 w/w ratio, using the suitable Cell Line Nucleofector kit (Lonza) and the Nucleofector II system (Amaxa Biosystem, now owned by Lonza). After transfection, cells recovered for 24 hours at 37 °C, 5% CO_2, in 2 ml of their usual culture medium. Cell viability was measured and cells were lysed for measurement of both firefly and *Renilla* luciferase activities with the Dual-Luciferase Reporter Assay System (Promega) on the Infinite M200 plate reader (Tecan Group Ltd, Männedorf, Switzerland) according to the manufacturer's instructions.

For data analysis, the ratio of *Renilla* luciferase activities between transfections using the IRE(−) or IRE(+) forms of the pGL3 plasmid was calculated. Data from these transfections were considered only if the *Renilla* luciferase ratio between the two experiments was 1 ± 0.25 to guaranty similar transfection efficiencies. The firefly luciferase activity for both IRE orientations was normalized to the *Renilla* one. The firefly luciferase activities were reported to the cell number or the protein concentration in the cell lysate. It must be stressed that other mRNA structures, particularly those devoid of a stem-loop, upstream of the sequence encoding F-*luc*[21–23] can hardly be compared with IRE-containing ones. Indeed, preliminary experiments indicated that the luciferase activity measured with the transfected pGL3-control plasmid was higher than the activity generated by any of the IRE- or reverse complementary IRE-containing plasmids. Thus, taking the pGL3-control plasmid as reference would enhance the apparent repression of the IRE-containing mRNA by IRP, but this enhanced repression would neglect the structural differences between the constructions being compared.

Table 2 IRE (+) sequences cloned upstream of the F-*luc* cDNA to regulate the luciferase activity as a function of IRP binding

Gene (alternate name)	[a]	IRE sequence[b]
FTH1	5′	**AGCTT*GGGTTTCC* TGC *TTCAA*CAGTGC*TTGGA*CGGAAA*CCC*TCTAGA**
FTL	5′	**AGCTTCTGTC*TCT*TGC*TTCAA*CAGTGT*TTGGA*CGGA*A*CAGATCTAGA**
ACO2	5′	**AGCTTGGG*TCAT*C*TTTGT*CAGTGC*ACAAAATGG*CCCTCTAGA**
EPAS1 (HIF2α)	5′	**AGCTT*GGGTACAAT*CCTCGGCAGTGT*CCTGAGAC*TGTACCC*TCTAGA**
ALAS2	5′	**AGCTT*GGGGTT*CGTCCTCAGTGC*AGGGCAACCCC*TCTAGA**
SLC11A2 (DMT1)	3′	**AGCTT*GCCATCAGAGCCAGTGT*GTTTC*TATGGT*CTAGA**
SLC40A1 (FPN1a)	5′	**AGCTTTCC*AACTTCAGCTACAGTGT*TAGCTAAGTTT*TGGAAAGTCTAGA**
CDC14A	3′	**AGCTT*GGGATATTTACATGTACAGTGT*TACATTATATATCCC*TCTAGA**
TFRC(b)	3′	**AGCTT*GGGATTATCGGAAGCAGTGC*CTTCCATAATCCC*TCTAGA**
AHSP	3′	**AGCTTGGGCAAT*AAAGACCAGTGC*TGGTTTT*GTTGCCCTCTAGA**

[a] Position of the IRE relative to the coding sequence of the gene in the human genome. [b] The predicted loop and unpaired bases of the stem (bulge) are underlined, the sequences predicted to be involved in stems are italicized.

Results

Enhancement of the activity of the Iron Regulatory Proteins in models of myelogenous leukemic cells

It was established long ago that iron deprivation enhances the IRP activity in metazoan cells.[24–26] The conventional growth medium used for K562 and KG1 cells provides largely enough iron for proliferation, although such cells display residual IRE-binding activity (Fig. 1A). Exposing these cells to large concentrations, *e.g.* 200 μM, of iron chelators such as DFO stops growth. Here, the DFO treatment was carried out for 24 h since longer exposure resulted in cell death.[13] Iron withdrawal by DFO is expected to enhance the IRE-binding activity of IRP, but, likely, in different proportions depending on the cell model and the growth conditions. In K562 cells, the IRP activity was significantly multiplied by 2.1 fold between DFO-treated and growing cells (Standard Deviation (SD) = 0.4, Student *t*-test $p < 0.001$), similar to KG1 cells, 2.2 fold (SD = 0.5, Student *t*-test $p < 0.019$) (Fig. 1A and B). The activity contributed by IRP1 arises from a fraction of the total IRP1 protein, and a strong reducing agent converts all of the protein present in cell lysates into the IRE binding form.[11,27] By adding 2% 2-mercaptoethanol (2ME) to the IRP-IRE binding assays, it was found that the activated (IRE-binding) IRP1 amount was similar to that obtained upon treating cells with DFO for 24 h before lysis (not shown). Therefore, addition of a chelator such as DFO to the growth medium enhances the cellular IRP activity in a similar proportion as addition of 2ME does for cell lysates. This implies that, even though the IRP2 protein should be stabilized by DFO, its contribution in the studied iron-depleted cells does not change the total activity revealed *in vitro* by 2ME in growing iron-replete cells.

Quantitative analysis of Iron Regulatory Proteins in models of myelogenous leukemic cells

The organization and impact of the IRP network necessarily rely on the actual amounts of the regulators and targets in cells. The endogenous IRP content was determined both by quantitative Western blots and by quantitative REMSA, with the use of pure recombinant human IRP1[11] as a reference. In six separate immuno-detection experiments such as (Fig. 1C), the IRP1 concentration was determined at 0.7 μM (SD = 0.5) for K562 cells growing in complete medium. IRP2 was not detected in these cells as expected,[2,3] since the protein is degraded under the iron-replete conditions used to grow them.[13] The limited involvement of IRP2 in proliferating K562 cells was confirmed by running Western blots with up to 40 μg of cell lysates, using either commercially available antibodies (Experimental), or locally produced ones against the purified specific IRP2-domain[12] as antigen. The latter antibodies have been validated using other cells.[15] Similar estimates of the IRP1 concentration in KG1 cells gave a shifted, but overlapping, value of 1.7 μM (SD = 1.5). In both cell lines treating cells with DFO did not significantly change the amount of the IRP1 protein as compared to the conventional growth medium.

The amount of IRP present in cells can alternatively be estimated by measuring the IRE-binding activity in experiments

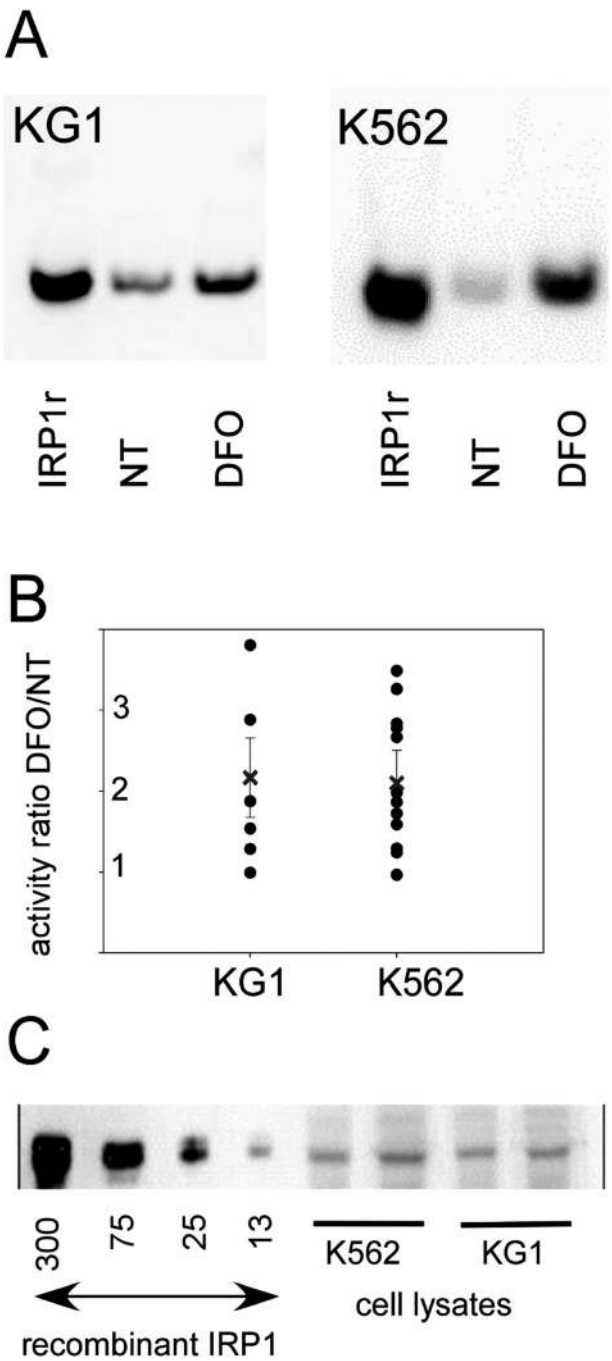

Fig. 1 Quantification of IRP in KG1 and K562 cells. (A) IRP-IRE interaction signal obtained by RNA electrophoretic mobility shift assays. Known amounts of recombinant IRP1 and of cell lysates were loaded on the same gel and band intensities were measured. The representative assays shown here used extracts prepared from cells grown in conventional medium (NT for not treated) or from cells exposed to 200 μM deferoxamine for 24 hours (DFO). (B) Ratios of IRP activities of individual samples (circles) treated with DFO as described in Experimental and samples of the same culture left without treatment. The dot plot gathers measurements with KG1 and K562 cells, carried out as in panel A. The crosses and error traces represent means and standard deviations of the data, respectively. (C) Representative quantitative Western Blot used to estimate IRP concentrations in cell lysates with recombinant IRP1 (ng) as standards. In this experiment, 10 (left lanes) and 20 μg (right lanes) of protein extracts of each indicated cell line were loaded on the gel.

similar to those shown in Fig. 1A with recombinant human IRP1 used to scale the data. Recombinant IRP1 was produced as previously described,[11] and it is the intact human protein with all residues expected from the sequence.[28] By doing so, concentrations of 1.6 and 1.9 μM in K562 and KG1 cells, respectively, were obtained with respective SD of 0.6 and 1.3.

Although the dispersion of the values is large when combining the results of many experiments, the means of active IRP and of the IRP1 protein return concentrations close to 1–2 μM, thus values in the μM range will be used for comparisons in the following.

The transcriptional profiles of the IRP targets and other relevant genes

IRP bind to several mRNA at the IRE sites. Yet, detailed studies[29] showed that only a minority of potential IRP mRNA-targets together (i) bind to IRP, (ii) are regulated by iron availability, and (iii) are sensitive to IRP depletion. Here, a set of the most validated IRP interactors (the mRNA of FTH1, FTL, TFRC, ALAS2, ACO2, and EPAS1, see Table 1 for nomenclature) was measured by reverse transcriptase-quantitative polymerase chain reaction (RT-qPCR) in order to estimate the relative proportions of the endogenous IRP targets. The transcriptional profiles are very similar between both cell lines for most studied genes (Fig. 2). The ferritin transcripts are the most abundant mRNA among the studied IRP targets, and they are more abundant in K562 than in KG1 cells, by the statistically significant factors of *ca.* 2.8 and 6 fold for the means of the H and L subunits, respectively. This result is not surprising in view of the different iron requirements of these two cell lines.[13] Indeed, ALAS2 and the globin transcripts were not reliably detected in KG1 cells, whereas they were easily measured in K562 cells which indicates that the K562 cell line produces more hemoglobin than KG1 cells. The high level of γ-globin expression, which increases upon hemin-induced maturation, has been previously evidenced in K562 cells.[30] Other genes, such as those encoding TFRC and the IRE-devoid ones, such as heme oxygenase 2 (constitutive isoform, HMOX2) and both IRP (ACO1 and IREB2), are similarly expressed in both leukemic models. This occurs in the absence of significant inducible heme oxygenase HMOX1 in K562 cells, in contrast to the small but measurable amount present in KG1 cells.

In order to get absolute concentrations of the above mRNA, similar experiments were carried out by spiking the RNA preparations with non-mammalian mRNA of known concentrations, as detailed in the Experimental section. The results of these determinations are reported in Table 3 as cellular mRNA concentrations to allow easy comparison with protein concentrations. Although the spreading of these values is large, with SD being *ca.* 50% of the reported values on average, these data provide fair estimates of the absolute concentrations of the mRNA in the studied cell lines. It thus appears that the IRE-bearing IRP targets have concentrations below 100 nM, *i.e.* at least one order of magnitude smaller than the concentration of the IRP (Fig. 1), and the sum of all such IRP-binding mRNA is far lower than the IRP concentration.

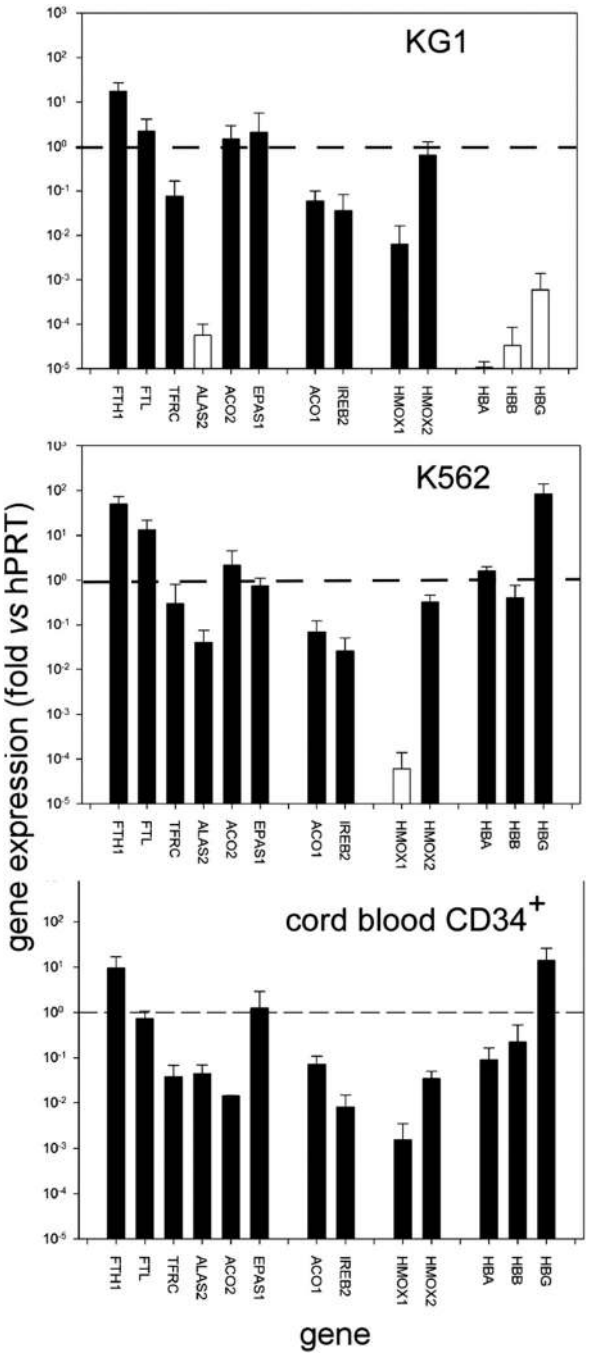

Fig. 2 Relative expression of genes of iron homeostasis in hematopoietic progenitors and leukemic models. Mean transcript expression (bars) relative to the reference gene hPRT with SD (lines). Top: KG1 cells. Middle: K562 cells. Bottom: $CD34^+$ cord blood cells after cell sorting (quiescent cells; $n = 2$). The dashed lines indicate the level of the hPRT reference. The white bars represent transcripts of vanishingly low concentrations that are not considered as efficiently expressed.

Tentative measurements of other potential IRP targets such as the IRE-binding forms of SLC40A1 (ferroportin) or SLC11A2 (DMT1) also returned values far below 1 nM, *i.e.* of marginal quantitative significance as compared to the ferritin subunits (Table 3) for instance.

Table 3 Average absolute concentrations (nM) of selected mRNA in KG1 and K562 cells

Gene	KG1	K562	Cord blood CD34+**
FTL	4.5	15	1.1
FTH1	32	65	14.6
TFRC	0.16	0.4	0.06
ACO2	2.7	3.3	0.022
ALAS2	*	0.06	0.07
ACO1	0.1	0.1	0.11
IREB2	0.08	0.04	0.013
HBA	*	2.2	0.14
HBB	*	0.6	0.34
HBG	*	125	21

Concentrations were calculated from qPCR amplification plots obtained by spiking the purification and RT steps of the RNA manipulations with known amounts of β-gal and F-*luc* synthetic mRNA (see Experimental). The resulting C_q were converted to concentrations in at least 6 independent experiments for each cell line, except for the haemoglobin subunits for which only 3 measurements were carried out. The blank line separates the transcripts interacting with IRP (above) from those that do not contain IRE (below). * The levels of the amplified products were too low to provide reliable determinations. ** The values indicated for progenitors were calculated from the data used to draw Fig. 2, assuming a similar level of reference genes in the different cells.

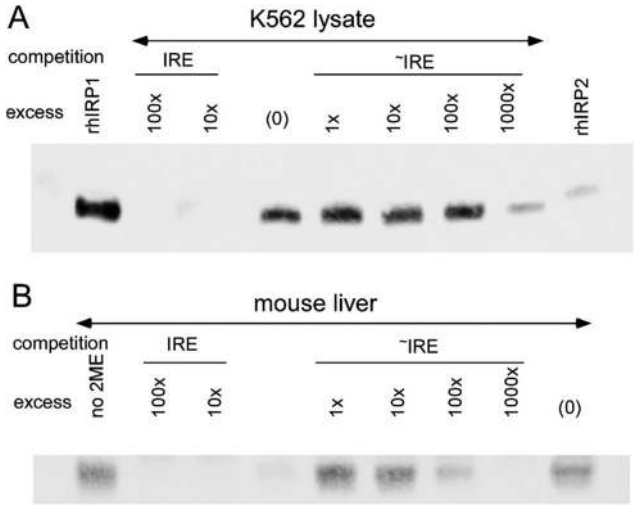

Fig. 3 Competition between the IRE FTH1 sequence and its reverse complement for binding to IRP. (A) REMSA of K562 lysates with labeled IRE from human FTH1. Either the same non-labeled IRE (wells 2 and 3) or the non-labeled reversed complementary IRE (∼IRE) were added to the assays in the indicated stoichiometric ratios. (0) indicates no addition of non-labeled competitor. Recombinant human IRP1 and IRP2 (rhIRP) were loaded in the side wells, left and right, respectively. (B) A similar competition experiment carried out with extracts of mouse liver with the indicated excess of either non-labeled FTH1 IRE (left wells) or the non-labeled reversed complementary ∼IRE (right wells).

These data were obtained with two selected cell lines, thus the experiments were extended to primary cells. Hematopoietic progenitors isolated from cord blood displayed a pattern of gene expression qualitatively similar to that of the cell lines, of K562 cells in particular (Fig. 2). Thus, despite the expected differences between primary cells and transformed cell lines, the expression of the main genes participating to cellular iron homeostasis is conserved.

Efficiency of the Iron Regulatory Proteins to repress translation *via* Iron Responsive Elements

The relative efficiencies of the endogenous IRP system to control different transfected IRE-*luc* constructions were then recorded. Two plasmids were built for each tested IRE (Table 2). The IRE sequences were cloned immediately upstream of the sequence encoding F-*luc* on the pGL3-control plasmid. Constructions bearing the IRE sequence in both directions were selected by sequencing, so that one, IRE 5′ → 3′ upstream of F-*luc*, could be recognized by IRP, whereas the other, the reverse complementary IRE sequence, could not, despite being probably folded similarly to IRE with a stem-loop structure. The inability of the IRP to recognize the reverse complementary IRE was experimentally verified in competition REMSA assays: these assays were carried out with K562 lysates, mouse liver extracts (Fig. 3), recombinant human IRP1 and IRP2, and lysates from the non-hematopoietic (insulinoma) INS-1 cell line (not shown). Loss of the shifted band corresponding to the IRE–IRP complex occurred with excess above 100 fold of the reverse complementary IRE sequence (∼IRE) over the labeled IRE probe, whereas a mere 10 fold excess of unlabeled genuine IRE fully erased the signal (Fig. 3). Thus, the plasmid bearing the wrongly oriented IRE sequence does not efficiently bind IRP, and it thus provides a convenient negative control, with a similar folding of the stem-loop structure, to the correctly oriented one.

To evaluate the variations of the amounts of IRE-bearing mRNA after transfection, RT-qPCR experiments were carried out with RNA prepared from the cell lines transfected with the IRE-F-*luc* constructions. The level of the luciferase mRNA was approximately that of hPRT. As compared to the RT-qPCR experiments reported above, the quantities of mRNA belonging to the iron network did not vary significantly, implying that transfection did not disturb their transcription (Fig. 4).

Since IRP binding should repress the firefly luciferase activity in cells transfected with the plasmid bearing the IRE in the correct orientation, designated IRE(+), the data are reported with this *Renilla* luciferase-normalized value as denominator. The numerator is the corresponding value for the plasmid with the same RNA sequence cloned in the reversed direction, IRE(−). Thus, IRP binding and repression is detected as a value of *Renilla*-normalized firefly luciferase activity ratio >1 for the IRE(−)/IRE(+) constructions.

This IRE(−)/IRE(+) ratio was measured for the IRE listed in Table 2 in the two different cell lines, K562 and KG1. The mean values and SD were not significantly different between these two cell lines, which agrees with the similar concentrations of IRP and of the main IRE-bearing mRNA measured above (Table 4). The largest ratios were for the IRE of erythroid aminolevulinate synthase (ALAS2), of mitochondrial aconitase (ACO2), and of the IRE-bearing splicing form of ferroportin (SLC40A1; FPN1a). The repression of the IRE of hypoxia inducible factor 2α (EPAS1), of the ferritin subunits (FTH1, FTL),

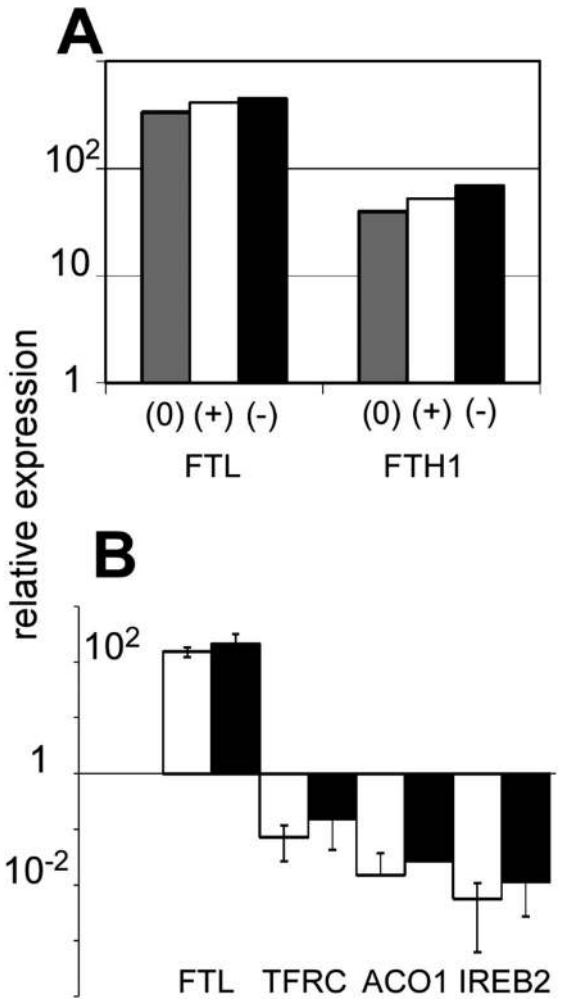

Fig. 4 Impact of cell transfection on transcript expression. (A) Relative expression of the ferritin transcripts in K562, not transfected (0), or transfected with the FTH1 IRE(+), and FTH1 IRE(−) constructions. (B) Relative expression of some transcripts in KG1 cells transfected by EPAS1 IRE(+) (white bars) or EPAS1 IRE(−) (black bars) constructions.

Table 4 Ratios of firefly luciferase activities in IRE(−) and IRE(+) transfected cell cultures

	KG1		K562	
IRE(−)/IRE(+)	Growing	DFO	Growing	DFO
FTH1	0.9 (0.07)	0.5 (0.5)	3.7 (2.6)	2.4 (2.1)
FTL	1.1 (0.09)	2.3 (0.8)	1.5 (0.4)	1.4 (0.1)
SLC40A1 (FPN1a)	3.6 (2.3)	4.1 (1.9)	4.5 (1.5)	3.4 (0.4)
SLC11A2 (DMT1)	2.1 (1.1)	1.1 (0.3)	1 (0.1)	1.0 (0.3)
ACO2	2.9 (0.8)	3.4 (0.7)	5.4 (2.5)	6.3 (3.0)
EPAS1 (HIF2α)	1.7 (0.7)	1.3 (0.6)	3.1 (2.3)	0.9 (0.6)
ALAS2	5.0 (1.1)	7.0 (2.4)	3.5 (1.9)	6.7 (4.9)

The reported ratios are the mean and SD (within brackets) of at least 3 independent experiments. ''Growing'' means that cells were transfected after being kept in the complete growth medium, ''DFO'' means that they were treated for 24 h by 200 μM DFO with evidence of growth arrest and enhanced IRP activity (Fig. 1) before transfection. The activities values were normalized to the protein concentration of the lysates and to the *Renilla* luciferase activity for transfection efficiency. Experiments in which any of these two parameters differed by more than 25% were rejected.

and of the IRE-bearing forms of the divalent metal transporter (SLC11A2, DMT1) was weak. Last, the constructions with the second IRE of the transferrin receptor 3′UTR (TFRC(b)), that of the α–hemoglobin stabilizing protein (AHSP), and of the cell division cycle 14A (CDC14A) failed to evidence any reliable decrease of the luciferase activity, and they were not studied further.

The above data were obtained after transfecting cells growing in complete medium. As the IRP system is sensitive to iron availability, cells were also deprived of iron by adding DFO for 24 h, so as to stop proliferation,[13] before transfection with the IRE-bearing plasmids. It has been show above (Fig. 1A and B) that this DFO treatment enhances the IRP activity by a factor close to 2. The enhancement of the endogenous IRP activity did not translate into any significantly larger repression of the luciferase activity with any of the studied IRE-*luc* constructions (Table 4). This is taken as evidence that the exogenous IRE is not sensitive to the *ca.* 2 fold-increased IRP activity in the present experimental conditions. This conclusion is further borne out when treating cells with other anti-proliferative agents replacing DFO. Cytarabine (1 μM) was used on KG1 cells and hydroxyurea (200 μM) on K562 cells to stop proliferation. Neither of these two compounds changed the ordering of the ratios of firefly luciferase activities measured with cells under normal growth conditions (data not shown).

Discussion

The above series of experiments provides one of the first cellular datasets describing the quantitative features of the IRP-IRE regulatory system. Manipulation of iron provision revealed all of the IRE-binding activity present in K562 and KG1 cells, as did *in vitro* unmasking of the total activity by reductive unfolding with 2ME. This behavior was expected from the currently accepted model of the modulation of IRP activity,[2] and the present experiments indicate that approximately half of IRP is under its IRE-binding form in these proliferating cell lines under laboratory conditions.

Quantification of IRP1 by Western Blots and REMSA calibrated with the pure recombinant protein allowed us to estimate the concentration of this regulator in the studied cells. Although these determinations varied between different experiments, the values fell always in the same range, around 1 μM. This is orders of magnitude larger than any of target mRNA bearing IRE, which were quantified largely below the 0.1 μM limit, with the ferritin subunits being by far the most abundant IRE-bearing transcripts. Of note, the far higher concentrations of proteins on average as compared to transcripts is a general trend of mammalian cells.[31,32] One may argue that our measurements are flawed in the estimates of proteins or mRNA. However, human IRP1 was purified to homogeneity and its concentration was determined both by conventional spectrophotometric protein assays and by measurement of the absorbance of the iron–sulfur cluster at *ca.* 400 nm since it is purified as cytosolic aconitase.[11] Furthermore, this material crystallized,

and the resulting structure comprised all amino acids predicted from the genomic sequence.[28] In the case of mRNA the calibration of each critical step of the quantification procedure with pure exogenous and synthetic transcripts minimized the error associated with these measurements (Experimental). Therefore, from the present data, it may be inferred that the amount of IRP largely exceeds the sum of all IRE mRNA, unless one considers many of the latter remain to be identified. Given the availability of the human genome sequence, the potency of deep sequencing, and the efficiency of the developed computer programs to screen for specific sequences (the structurally well conserved IRE sequences in the present case), the occurrence of many more conventional IRE-mRNA than the presently known dozen seems unlikely. Indeed, the already identified IRE constituted the majority of the mRNA interacting with IRP,[29] even though other stem-loop mRNA structures may interact with IRP in other cell types.[2]

The large excess of the IRP regulator over any of its regulated mRNA targets is further borne out by previous measurements carried out with a significant fraction of the transcriptome and proteome of a mouse fibroblast cell line.[18] The amount of the IRP1 protein (the product of the ACO1 gene), after correction,[31,32] was close to that estimated here, despite the use of another cell model from another species. Along the same lines, the fraction of RNA-bound IRP1 in other cellular contexts was estimated to be small although the conformation of the protein responded to conditions such as anemia or type I hereditary hemochromatosis.[33]

In HeLa cells, manipulations of the amounts of both IRP by siRNA technology established that loss of IRP regulation on ferritin and transferrin receptor messengers could only be observed when the remaining mRNA of IRP was only a few % of the concentration before knock-down and corresponding to undetectable amounts of the IRP.[23] These data are in agreement with the IRP/IRE ratio of 10 or more estimated in the present study. In other words, the regulation by IRP is maintained with a minority of the IRE-binding capacity present in these cells. One may argue that other post-transcriptional regulation mechanisms may be at work, such as those involving micro RNA or small interfering RNA, but these would not re-equilibrated the IRP/IRE ratio since they decrease the concentration of targeted messengers, and their contribution has been implicitly taken into account in our experimental approach.

All the above converging data lead to conclude that IRP may be distinguished from other well characterized mRNA-binding proteins. The AU-rich element binding protein HuR, for instance, displays a wealth of targets and a relatively simple and abundant recognition motif,[34] whereas genuine IRE are long (>30 nt) RNA sequences folding as stem-loop structures which are far less frequent genome-wide. Significantly, IRP often escape the modern screenings methods of RNA-binding proteins.[17,35,36]

Available results addressing the dissociation constants (K_d) for binding of IRP to IRE *in vitro* are discrepant, with values in the pM range[37–39] up to the nM one.[40] The divalent metal dependence of this dissociation constant may contribute to the inconsistencies.[41] K_d values in the pM–100 nM range would leave a large concentration of the IRP we measured (≈ 1 μM) free to interact with additional IRE. Yet, transfection of KG1 and K562 cells with plasmids encoding firefly luciferase under the dependence of various naturally occurring IRE led to very limited IRP regulation, and none for some of these IRE (Table 4), despite the amount of *luc* mRNA being measured within the range found for endogenous IRE-bearing transcripts (Fig. 4). This contrasts with most previous work implementing a similar strategy with other cell models[21–23] but with questionable referencing (see Experimental). Thus, very little of the IRP present in transfected cells could be mobilized to bind to the added IRE. The difference may be due to factors that seem to modulate the IRP activity inside cells, such as physiological divalent metal ions and potentially competitive IRE-binding proteins,[41] or the role ribosomes or mRNA structures, *e.g.* the cap,[42] may play in the IRP–IRE interaction. All these elements are not interfering in the *in vitro* experiments used to derive K_d values.[38,40]

Conclusions

Modulation of IRP activity does impinge on the phenotype of animal systems. Mice devoid of IRP1 displayed polycythemia, and those without IRP2 experienced microcytic anemia ([6] for review). Reciprocally, IRP1 gain of function also perturbed erythropoiesis.[43] Thus, the proper balance between the IRP and the different IRE is requested for normal hematopoiesis, and the quantitative data presented here may help progressing in understanding the detailed mechanisms at work in such situations. It can be noticed that the leukemic models studied herein display strong basal activation (*ca.* 50%) of the IRP regulator (Fig. 1A). Indeed, hematopoietic progenitors, and leukemic cells in particular, have high iron requirements for proliferation[44] and the iron needs during differentiation vary greatly depending on the lineage.[45,46] Hence leukemic clones may divert the regulatory IRP/IRE system for enhanced proliferation. Thus therapeutic options implementing chelators may efficiently target expanding clones, as observed in some instances of iron overload.[9,47,48] However, detailed mechanisms of action deserve scrutiny as recently exemplified in myelodysplastic syndromes[49] to efficiently and individually target hemopathies in an informed way. Combined with proper quantitative integration,[50,51] such details would also be relevant for the many other diseases in which iron dysregulation is thought to participate to the deleterious process and for which targeting of the IRE/IRP system is considered, *e.g.* ref. 52.

Conflicts of interest

The authors have no conflicts of interest to declare.

Acknowledgements

EP is the recipient of a grant from the *Société Française d'Hématologie* (SFH). Ghina El Samra is thanked for cord blood

RNA amplification. This work was supported by grants from Région Rhône-Alpes (Programme Cible 2010), Institut Rhône-Alpin des systèmes complexes (IXXI), Université Joseph Fourier Grenoble (Programme Agir 2013), Direction de la Recherche Clinique (DRC) CHU Grenoble, Ligue Nationale Contre Le Cancer (Projet Pluri Equipes), Plan Cancer – Biologie des systèmes édition 2017, and Novartis. The company played no role in the design and the interpretation of the results.

Notes and references

1 F. Gebauer and M. W. Hentze, Molecular mechanisms of translational control, *Nat. Rev. Mol. Cell Biol.*, 2004, **5**, 827–835.

2 J. Wang and K. Pantopoulos, Regulation of cellular iron metabolism, *Biochem. J.*, 2011, **434**, 365–381.

3 S. Recalcati, G. Minotti and G. Cairo, Iron regulatory proteins: from molecular mechanisms to drug development, *Antioxid. Redox Signaling*, 2010, **13**, 1593–1616.

4 K. Volz, The functional duality of iron regulatory protein 1, *Curr. Opin. Struct. Biol.*, 2008, **18**, 106–111.

5 M. U. Muckenthaler, B. Galy and M. W. Hentze, Systemic iron homeostasis and the iron-responsive element/iron-regulatory protein (IRE/IRP) regulatory network, *Annu. Rev. Nutr.*, 2008, **28**, 197–213.

6 D. L. Zhang, M. C. Ghosh and T. A. Rouault, The physiological functions of iron regulatory proteins in iron homeostasis – an update, *Front. Pharmacol.*, 2014, **5**, 124.

7 A. G. Hinnebusch, I. P. Ivanov and N. Sonenberg, Translational control by 5′-untranslated regions of eukaryotic mRNAs, *Science*, 2016, **352**, 1413–1416.

8 A. M. Zeidan, V. A. Pullarkat and R. S. Komrokji, Overcoming barriers to treating iron overload in patients with lower-risk myelodysplastic syndrome, *Crit. Rev. Oncol. Hematol.*, 2017, **117**, 57–66.

9 E. Paubelle, F. Zylbersztejn, S. Alkhaeir, F. Suarez, C. Callens, M. Dussiot, F. Isnard, M. T. Rubio, G. Damaj, N. C. Gorin, J. P. Marolleau, R. C. Monteiro, I. C. Moura and O. Hermine, Deferasirox and vitamin D improves overall survival in elderly patients with acute myeloid leukemia after demethylating agents failure, *PLoS One*, 2013, **8**, e65998.

10 E. Pourcelot, N. Mobilia, A. Donzé, F. Louis, O. Maler, P. Mossuz, E. Fanchon and J.-M. Moulis, in *Nutzen-Risiko-Bewertung von Mineralstoffen und Spurenelementen*, ed. A. Hartwig, B. Köberle and B. Michalke, KIT Scientific Publishing Karlsruhe, Germany, 2013, pp. 73–89, http://books.openedition.org/ksp/122.

11 X. Brazzolotto, J. Gaillard, K. Pantopoulos, M. W. Hentze and J. M. Moulis, Human cytoplasmic aconitase (Iron regulatory protein 1) is converted into its [3Fe–4S] form by hydrogen peroxide *in vitro* but is not activated for iron-responsive element binding, *J. Biol. Chem.*, 1999, **274**, 21625–21630.

12 C. Dycke, C. Bougault, J. Gaillard, J. P. Andrieu, K. Pantopoulos and J. M. Moulis, Human iron regulatory protein 2 is easily cleaved in its specific domain: consequences for the haem binding properties of the protein, *Biochem. J.*, 2007, **408**, 429–439.

13 E. Pourcelot, M. Lénon, N. Mobilia, J.-Y. Cahn, J. Arnaud, E. Fanchon, J.-M. Moulis and P. Mossuz, Iron for proliferation of cell lines and hematopoietic progenitors: Nailing down the intracellular functional iron concentration, *Biochim. Biophys. Acta*, 2015, **1853**, 1596–1605.

14 A. Martelli and J. M. Moulis, Zinc and cadmium specifically interfere with RNA-binding activity of human iron regulatory protein 1, *J. Inorg. Biochem.*, 2004, **98**, 1413–1420.

15 I. Ferecatu, S. Goncalves, M. P. Golinelli-Cohen, M. Clemancey, A. Martelli, S. Riquier, E. Guittet, J. M. Latour, H. Puccio, J. C. Drapier, E. Lescop and C. Bouton, The diabetes drug target MitoNEET governs a novel trafficking pathway to rebuild an Fe–S cluster into cytosolic aconitase/iron regulatory protein 1, *J. Biol. Chem.*, 2014, **289**, 28070–28086.

16 S. A. Bustin, V. Benes, J. A. Garson, J. Hellemans, J. Huggett, M. Kubista, R. Mueller, T. Nolan, M. W. Pfaffl, G. L. Shipley, J. Vandesompele and C. T. Wittwer, The MIQE guidelines: minimum information for publication of quantitative real-time PCR experiments, *Clin. Chem.*, 2009, **55**, 611–622.

17 A. G. Baltz, M. Munschauer, B. Schwanhausser, A. Vasile, Y. Murakawa, M. Schueler, N. Youngs, D. Penfold-Brown, K. Drew, M. Milek, E. Wyler, R. Bonneau, M. Selbach, C. Dieterich and M. Landthaler, The mRNA-bound proteome and its global occupancy profile on protein-coding transcripts, *Mol. Cell*, 2012, **46**, 674–690.

18 B. Schwanhäusser, D. Busse, N. Li, G. Dittmar, J. Schuchhardt, J. Wolf, W. Chen and M. Selbach, Global quantification of mammalian gene expression control, *Nature*, 2011, **473**, 337–342.

19 C. Strein, A. M. Alleaume, U. Rothbauer, M. W. Hentze and A. Castello, A versatile assay for RNA-binding proteins in living cells, *RNA*, 2014, **20**, 721–731.

20 C. Vogel, S. Abreu Rde, D. Ko, S. Y. Le, B. A. Shapiro, S. C. Burns, D. Sandhu, D. R. Boutz, E. M. Marcotte and L. O. Penalva, Sequence signatures and mRNA concentration can explain two-thirds of protein abundance variation in a human cell line, *Mol. Syst. Biol.*, 2010, **6**, 400.

21 R. J. Henderson, S. M. Patton and J. R. Connor, Development of a fluorescent reporter to assess iron regulatory protein activity in living cells, *Biochim. Biophys. Acta*, 2005, **1743**, 162–168.

22 J. Y. Li, G. Ram, K. Gast, X. Chen, K. Barasch, K. Mori, K. Schmidt-Ott, J. Wang, H. C. Kuo, C. Savage-Dunn, M. D. Garrick and J. Barasch, Detection of intracellular iron by its regulatory effect, *Am. J. Physiol. Cell physiology*, 2004, **287**, C1547–C1559.

23 W. Wang, X. Di, R. B. D'Agostino, Jr., S. V. Torti and F. M. Torti, Excess capacity of the iron regulatory protein system, *J. Biol. Chem.*, 2007, **282**, 24650–24659.

24 E. A. Leibold and H. N. Munro, Cytoplasmic protein binds *in vitro* to a highly conserved sequence in the 5′ untranslated region of ferritin heavy- and light-subunit mRNAs, *Proc. Natl. Acad. Sci. U. S. A.*, 1988, **85**, 2171–2175.

25 E. W. Müllner, B. Neupert and L. C. Kühn, A specific mRNA binding factor regulates the iron-dependent stability of cytoplasmic transferrin receptor mRNA, *Cell*, 1989, **58**, 373–382.

26 T. A. Rouault, M. W. Hentze, S. W. Caughman, J. B. Harford and R. D. Klausner, Binding of a cytosolic protein to the iron-responsive element of human ferritin messenger RNA, *Science*, 1988, **241**, 1207–1210.

27 M. W. Hentze, T. A. Rouault, J. B. Harford and R. D. Klausner, Oxidation–reduction and the molecular mechanism of a regulatory RNA-protein interaction, *Science*, 1989, **244**, 357–359.

28 J. Dupuy, A. Volbeda, P. Carpentier, C. Darnault, J. M. Moulis and J. C. Fontecilla-Camps, Crystal structure of human iron regulatory protein 1 as cytosolic aconitase, *Structure*, 2006, **14**, 129–139.

29 M. Sanchez, B. Galy, B. Schwanhaeusser, J. Blake, T. Bahr-Ivacevic, V. Benes, M. Selbach, M. U. Muckenthaler and M. W. Hentze, Iron regulatory protein-1 and -2: transcriptome-wide definition of binding mRNAs and shaping of the cellular proteome by iron regulatory proteins, *Blood*, 2011, **118**, e168–e179.

30 P. Charnay and T. Maniatis, Transcriptional regulation of globin gene expression in the human erythroid cell line K562, *Science*, 1983, **220**, 1281–1283.

31 J. J. Li, P. J. Bickel and M. D. Biggin, System wide analyses have underestimated protein abundances and the importance of transcription in mammals, *PeerJ*, 2014, **2**, e270.

32 B. Schwanhäusser, D. Busse, N. Li, G. Dittmar, J. Schuchhardt, J. Wolf, W. Chen and M. Selbach, Corrigendum: Global quantification of mammalian gene expression control, *Nature*, 2013, **495**, 126–127.

33 S. Recalcati, A. Alberghini, A. Campanella, U. Gianelli, E. De Camilli, D. Conte and G. Cairo, Iron regulatory proteins 1 and 2 in human monocytes, macrophages and duodenum: expression and regulation in hereditary hemochromatosis and iron deficiency, *Haematologica*, 2006, **91**, 303–310.

34 S. Lebedeva, M. Jens, K. Theil, B. Schwanhausser, M. Selbach, M. Landthaler and N. Rajewsky, Transcriptome-wide analysis of regulatory interactions of the RNA-binding protein HuR, *Mol. Cell*, 2011, **43**, 340–352.

35 A. Castello, B. Fischer, K. Eichelbaum, R. Horos, B. M. Beckmann, C. Strein, N. E. Davey, D. T. Humphreys, T. Preiss, L. M. Steinmetz, J. Krijgsveld and M. W. Hentze, Insights into RNA biology from an atlas of mammalian mRNA-binding proteins, *Cell*, 2012, **149**, 1393–1406.

36 Y. C. Yang, C. Di, B. Hu, M. Zhou, Y. Liu, N. Song, Y. Li, J. Umetsu and Z. J. Lu, CLIPdb: a CLIP-seq database for protein-RNA interactions, *BMC Genomics*, 2015, **16**, 51.

37 H. A. Barton, R. S. Eisenstein, A. Bomford and H. N. Munro, Determinants of the interaction between the iron-responsive element-binding protein and its binding site in rat L-ferritin mRNA, *J. Biol. Chem.*, 1990, **265**, 7000–7008.

38 J. B. Goforth, S. A. Anderson, C. P. Nizzi and R. S. Eisenstein, Multiple determinants within iron-responsive elements dictate iron regulatory protein binding and regulatory hierarchy, *RNA*, 2010, **16**, 154–169.

39 D. J. Haile, M. W. Hentze, T. A. Rouault, J. B. Harford and R. D. Klausner, Regulation of interaction of the iron-responsive element binding protein with iron-responsive RNA elements, *Mol. Cell. Biol.*, 1989, **9**, 5055–5061.

40 M. A. Khan, W. E. Walden, E. C. Theil and D. J. Goss, Thermodynamic and Kinetic Analyses of Iron Response Element (IRE)-mRNA Binding to Iron Regulatory Protein, IRP1, *Sci. Rep.*, 2017, **7**, 8532.

41 E. C. Theil, IRE mRNA riboregulators use metabolic iron (Fe(2+)) to control mRNA activity and iron chemistry in animals, *Metallomics*, 2015, **7**, 15–24.

42 M. Muckenthaler, N. K. Gray and M. W. Hentze, IRP-1 binding to ferritin mRNA prevents the recruitment of the small ribosomal subunit by the cap-binding complex eIF4F, *Mol. Cell*, 1998, **2**, 383–388.

43 D. Casarrubea, L. Viatte, T. Hallas, A. Vasanthakumar, R. S. Eisenstein, K. Schumann, M. W. Hentze and B. Galy, Abnormal body iron distribution and erythropoiesis in a novel mouse model with inducible gain of iron regulatory protein (IRP)-1 function, *J. Mol. Med.*, 2013, **91**, 871–881.

44 L. I. Zon, Intrinsic and extrinsic control of haematopoietic stem-cell self-renewal, *Nature*, 2008, **453**, 306–313.

45 J. L. Kramer, I. Baltathakis, O. S. Alcantara and D. H. Boldt, Differentiation of functional dendritic cells and macrophages from human peripheral blood monocyte precursors is dependent on expression of p21 (WAF1/CIP1) and requires iron, *Br. J. Haematol.*, 2002, **117**, 727–734.

46 N. M. Sposi, L. Cianetti, E. Tritarelli, E. Pelosi, S. Militi, T. Barberi, M. Gabbianelli, E. Saulle, L. Kuhn, C. Peschle and U. Testa, Mechanisms of differential transferrin receptor expression in normal hematopoiesis, *FEBS J.*, 2000, **267**, 6762–6774.

47 A. M. Merlot, D. S. Kalinowski and D. R. Richardson, Novel chelators for cancer treatment: where are we now?, *Antioxid. Redox Signaling*, 2013, **18**, 973–1006.

48 P. Armand, M. M. Sainvil, H. T. Kim, J. Rhodes, C. Cutler, V. T. Ho, J. Koreth, E. P. Alyea, E. J. Neufeld, R. Y. Kwong, R. J. Soiffer and J. H. Antin, Pre-transplantation iron chelation in patients with MDS or acute leukemia and iron overload undergoing myeloablative allo-SCT, *Bone Marrow Transplant.*, 2013, **48**, 146–147.

49 M. Meunier, S. Ancelet, C. Lefebvre, J. Arnaud, C. Garrel, M. Pezet, Y. Wang, P. Faure, G. Szymanski, N. Duployez, C. Preudhomme, D. Biard, B. Polack, J. Y. Cahn, J. M. Moulis and S. Park, Reactive oxygen species levels control NF-kappaB activation by low dose deferasirox in erythroid progenitors of low risk myelodysplastic syndromes, *Oncotarget*, 2017, **8**, 105510.

50 J. Chifman, S. Arat, Z. Deng, E. Lemler, J. C. Pino, L. A. Harris, M. A. Kochen, C. F. Lopez, S. A. Akman, F. M. Torti, S. V. Torti and R. Laubenbacher, Activated Oncogenic Pathway Modifies Iron Network in Breast Epithelial Cells: A Dynamic Modeling Perspective, *PLoS Comput. Biol.*, 2017, **13**, e1005352.

51 N. Mobilia, A. Donzé, J.-M. Moulis and E. Fanchon, Producing a Set of Models for the Iron Homeostasis Network, *Electronic Proceedings in Theoretical Computer Science*, 2013, **125**, 92–98.

52 Z. D. Zhou and E. K. Tan, Iron regulatory protein (IRP)-iron responsive element (IRE) signaling pathway in human neurodegenerative diseases, *Mol. Neurodegener.*, 2017, **12**, 75.